

Decisive role of interstitial defects in half-Heusler semiconductors

An ab initio study

Dey, Poulumi; Dutta, Biswanath

DOI

[10.1103/PhysRevMaterials.5.035407](https://doi.org/10.1103/PhysRevMaterials.5.035407)

Publication date

2021

Document Version

Final published version

Published in

Physical Review Materials

Citation (APA)

Dey, P., & Dutta, B. (2021). Decisive role of interstitial defects in half-Heusler semiconductors: An ab initio study. *Physical Review Materials*, 5(3), Article 035407. <https://doi.org/10.1103/PhysRevMaterials.5.035407>

Important note


To cite this publication, please use the final published version (if applicable).
Please check the document version above.

Copyright

Other than for strictly personal use, it is not permitted to download, forward or distribute the text or part of it, without the consent of the author(s) and/or copyright holder(s), unless the work is under an open content license such as Creative Commons.

Takedown policy

Please contact us and provide details if you believe this document breaches copyrights.
We will remove access to the work immediately and investigate your claim.

Decisive role of interstitial defects in half-Heusler semiconductors: An *ab initio* studyPoulumi Dey  and Biswanath Dutta **Department of Materials Science and Engineering, Faculty of Mechanical, Maritime and Materials Engineering, Delft University of Technology, Mekelweg 2, 2628 CD Delft, The Netherlands* (Received 8 December 2020; revised 12 February 2021; accepted 22 February 2021; published 22 March 2021)

Half-Heusler semiconductors satisfying 18-electron rule typically display promising characteristics for thermoelectric applications. A persistent inconsistency between the type of charge carriers in some of these alloys as obtained from experiment and theory however casts serious doubt on the computational prediction of new and efficient half-Heusler alloys. To gain insights into the origin of this disparity, we have investigated the effect of intrinsic point defects on the electronic structure of four frequently studied half-Heusler alloys of the form XYZ with Y being Ni or Co. Using state-of-the-art *ab initio* calculations, our study reveals that interstitial Ni and Co are energetically most stable point defects in these alloys. Remarkably, interstitial defect modifies the location of the Fermi level inside the band gap as well as the value of the band gap, thereby bringing in close agreement with the corresponding experimental result. This work thus highlights the decisive role played by interstitial defects in thermoelectric half-Heusler alloys, which may open a new avenue for deliberately utilizing these defects as a strategy for tailoring electronic structure and hence the corresponding thermoelectric properties.

DOI: [10.1103/PhysRevMaterials.5.035407](https://doi.org/10.1103/PhysRevMaterials.5.035407)**I. INTRODUCTION**

In the ongoing quest for materials that are capable of converting huge amount of available waste heat into valuable electrical energy [1–18], half-Heusler thermoelectric alloys [19–29] have lately attracted enormous attention. These alloys are ternary intermetallics with the three elements in 1:1:1 stoichiometric proportion as represented by the general formula XYZ (X and Y are transition metals and Z is nonmagnetic element) [30]. Among the many desirable properties, half-Heusler alloys exhibit good values of the thermoelectric figure of merit, robust mechanical properties, high-temperature stability and use low cost, nontoxic, and earth-abundant elements. In recent years, the experimental and theoretical observations of superior thermoelectric performance in alloys within this family having 18 valence electrons per unit cell have accelerated the search for new half-Heusler alloys fulfilling the 18-electron rule [24,28]. The valence electrons in these alloys occupy all bonding electronic states, while antibonding states remain unoccupied thereby leading to the semiconducting band gap. Examples of thermoelectric materials belonging to this class of alloys include $XNiSn$ and $XCoSb$ (where $X = Hf, Zr, Ti$) [31–37] and $NbCoSn$ -based alloys [38–41]. All the above mentioned half-Heusler alloys with a valence electron count of 18 are promising candidates for thermoelectric applications with large Seebeck coefficient of up to several hundred $\mu V K^{-1}$ and moderate electrical conductivity. Furthermore, the valence electron concentration in these alloys can be tuned by the partial substitution of elements occupying the three available sites.

In spite of the existence of plethora of studies on half-Heusler thermoelectric materials, a fundamental discrepancy

remains between state-of-the-art theoretical and experimental findings. This discrepancy is manifested in terms of the theoretical prediction of some of the undoped n-type narrow band gap half-Heusler alloys as p-type semiconductor. For instance, the *ab initio* electronic band structure calculations performed within the density functional theory (DFT) framework predicted $NbCoSn$ to be a p-type semiconductor [39], while experimental measurements found the alloy to be intrinsically n-type [40–42]. Similarly, the Seebeck coefficient measurements for $ZrNiSn$ and $HfNiSn$ [43–45] confirmed these alloys to be n-type semiconductors. The *ab initio* band structure calculations, on the contrary, predicted these half-Heusler alloys to be p-type in nature [46]. Other half-Heusler alloys for which such a discrepancy exists between band structure calculations [47,48] and experimental measurements [49–51] include $TiNiSn$ and $TiCoSb$. For understanding and tailoring electronic band structure in a controlled manner to improve the thermoelectric performance of half-Heusler alloys, resolving the above discrepancy between theoretical and experimental findings is of pivotal importance.

It is noteworthy that most of the previous *ab initio* investigations considered defect-free stoichiometric composition for half-Heusler alloys. However, the half-Heusler alloys have been found to be prone to chemical off-stoichiometry [52,53]. The intrinsic point defects resulting in off-stoichiometric compositions have been previously reported for several half-Heusler alloys such as $TiNiSn$ [54–57], $HfNiSn$ [58,59], and $ZrNiSn$ [33,60,61]. For instance, analyzing the Seebeck coefficient of $TiNiSn$ using the Goldsmid-Sharp formula [62], Barczak *et al.* [63] reported gradual reduction in the band gap with increasing amount of interstitial defect. In good agreement with this finding, *ab initio* studies showed that the structural interstitial defects reduce the band gap of $TiNiSn$ [57,64,65]. These findings for $TiNiSn$ indicate that intrinsic defects may, in general, play decisive role in determining the

*Corresponding author: b.dutta@tudelft.nl

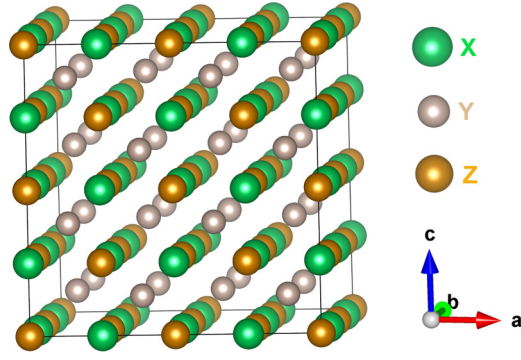


FIG. 1. Schematic representation of the cubic $C1_b$ crystal structure adopted by half-Heusler alloys (space group $F\bar{4}3m$).

type of charge carriers and band gap of the above-mentioned half-Heusler alloys and help in solving the long-standing discrepancy between theoretical predictions and experimental observations for similar n-type half-Heusler alloys.

The purpose of this paper is to underscore the general impact of intrinsic point defects on the electronic structure of the n-type Co- and Ni-based half-Heusler alloys. In order to achieve an in-depth understanding, we carry out thorough DFT-based investigations of the defect energetics and the subsequent effect on the electronic structure in four widely studied narrow band gap half-Heusler alloys viz. NbCoSn, TiCoSb, ZrNiSn, and TiNiSn. Our calculations make an interesting revelation that the p-type behavior theoretically predicted earlier for the above stoichiometric half-Heusler alloys changes to n-type with the consideration of intrinsic point defects. Our results are, thus, in agreement with the experimental observation, explaining the n-type nature and the band gap of each of the above mentioned half-Heusler alloys. To the best of our knowledge, the present study is first of its kind highlighting the significance of intrinsic point defects for deriving correct electronic structure within the DFT framework for both Co- and Ni-based n-type half-Heusler alloys.

The rest of the paper is organized as follows. In the following section, all details on the DFT simulations are provided. In Sec. III, the results on defect formation energies and electronic structure are presented along with the corresponding discussion. Finally, in Sec. IV, the main conclusions of our work are summarized.

II. COMPUTATIONAL METHODOLOGY

The underlying $C1_b$ crystal structure (MgAgAs-type with space group $F\bar{4}3m$) of the half-Heusler alloys with general formula XYZ can be visualized as an XZ rock salt sublattice with half of the tetrahedral sites being occupied by Y as shown in Fig. 1. We perform theoretical calculations using DFT [66,67] as implemented in the Vienna *ab initio* Simulation Package (VASP) [68–70]. The total energies and forces are calculated using the projector augmented wave method [71] together with the generalized-gradient approximation (GGA) for the exchange-correlation potential parametrized by Perdew, Burke, and Ernzerhof (PBE) [72]. The single-electron wavefunctions are expanded using plane waves up to an energy cutoff of 500 eV. An energy tolerance of 10^{-7} eV is

used as a convergence criterion for the self-consistent electronic loop. All lattice parameters and atomic positions are relaxed until the residual forces acting on each atom are below 0.0001 eV \AA^{-1} . Such strict choice of cutoff parameters and convergence criteria result in DFT energies with an error ≤ 0.1 meV atom^{-1} . The defect formation energies and electronic band structures are calculated for $2 \times 2 \times 2$ supercells comprising 96 atoms as illustrated in Fig. 1. For the vacancy formation, one of the 96 atoms is replaced by a vacancy, while for the interstitial defect, an additional atom is placed in the vacant $4d$ site of the $C1_b$ crystal structure. The interstitial defect leads to approximately 3% excess concentration of the element occupying the defect site. For the Brillouin-zone sampling, the tetrahedron method [73] with a k -point grid of $8 \times 8 \times 8$ is employed. A dense k -point grid of $14 \times 14 \times 14$ is used for the calculation of density of states (DOS).

III. RESULTS

A. Intrinsic point defects

We begin investigations by calculating formation energies of intrinsic point defects, i.e., vacancies, interstitials, and antisites, of the half-Heusler alloys NbCoSn, TiCoSb, ZrNiSn, and TiNiSn at 0 K. The point defect formation energies can be estimated [74] from the following equations:

$$\Delta E(I_\alpha) = E(\text{defect}) - E(\text{perfect}) - \mu_\alpha, \quad (1)$$

$$\Delta E(V_\alpha) = E(\text{defect}) - E(\text{perfect}) + \mu_\alpha, \quad (2)$$

$$\Delta E(\beta_\alpha) = E(\text{defect}) - E(\text{perfect}) + \mu_\alpha - \mu_\beta, \quad (3)$$

where $\Delta E(V_\alpha)$ and $\Delta E(I_\alpha)$ denote formation energies of a vacancy and an interstitial defect of atom α , respectively. $\Delta E(\beta_\alpha)$ is the antisite formation energy of atom β replacing atom α . $E(\text{perfect})$ and $E(\text{defect})$ are the total energies of the system without any defect and containing a defect respectively. μ_α denotes chemical potential of the atom α . In the present study, we have chosen bulk ground state energies per atom of elemental solids as their chemical potentials.

Figure 2 shows theoretically estimated point defect formation energies of the four half-Heusler alloys. Previous *ab initio* calculations for TiNiSn predicted Ni interstitial to be the most stable point defect in the alloy [57,64,65]. A comparison of the calculated and X-ray photoemission spectroscopy measured DOS further provided indirect evidence that excess Ni atoms occupy vacant $4d$ sites in the $C1_b$ TiNiSn alloy [75]. Our calculations using equations (1)–(3) indicate that Ni interstitial is energetically the most favorable defect with lowest formation energy in both Ni-based alloys, i.e., ZrNiSn and TiNiSn [Figs. 2(c) and 2(d)]. The formation energies of other point defects are significantly higher than the Ni interstitial formation energy. For Co-based alloys, i.e., NbCoSn and TiCoSb, the formation energies of interstitial Co defect are slightly higher than those for the Ni interstitial in Ni-containing alloys. Nonetheless, interstitial Co is the most abundant defect among all intrinsic point defects in these two alloys [Figs. 2(a) and 2(b)]. This indicates that excess Ni and Co atoms, due to their smaller atomic radius than other chemical elements in

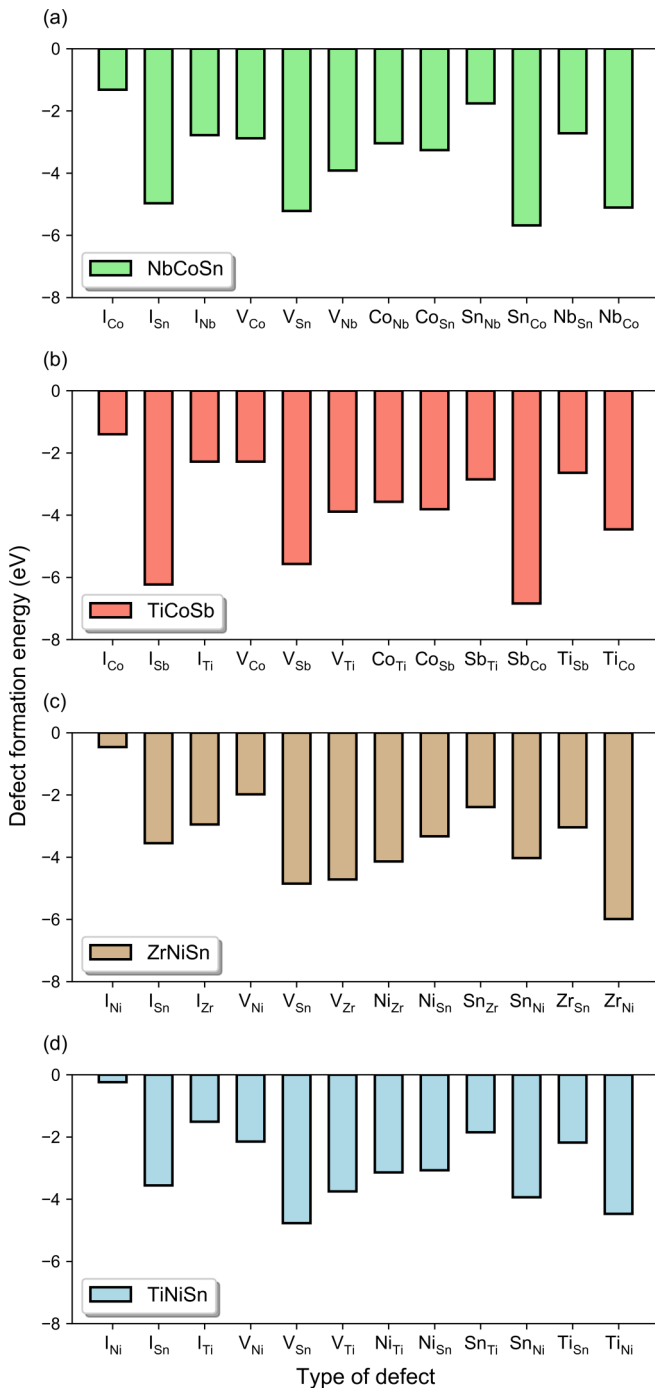


FIG. 2. *Ab initio* computed formation energies of various defects in (a) NbCoSn, (b) TiCoSb, (c) ZrNiSn, and (d) TiNiSn at 0 K.

the above Ni- and Co-based alloys, are more likely to occupy vacant interstitial sites. Our study of intrinsic point defects for the half-Heusler alloys can also be interesting in the context of full-Heusler thermoelectric materials for which such defects are found to play decisive role in determining their thermoelectric performance [76–79].

Note that our calculations indicate different magnetic properties for the two interstitial defects, i.e., Ni and Co. While Ni interstitial is nonmagnetic in nature, interstitial Co defect is stabilized in a ferromagnetic state in both NbCoSn and

TiCoSb. Without interstitial defects, all four alloys are non-magnetic. The effect of different magnetic states exhibited by the interstitial defects on the corresponding DOS is discussed later in the paper.

B. Electronic band structure and density of states

Unlike the usual tendency to predict underestimated band gap in solids [80–84], *ab initio* calculations yielded higher values of band gap in comparison to experimentally measured values for the above-mentioned half-Heusler alloys [48,85–87]. It has been speculated that slight change in alloy composition in the experimental samples due to point defects may explain this deviation from the usual trend observed in semiconductors [57,64,65]. While external doping is the commonly employed point defect engineering strategy for tailoring carrier concentration and mobility [44–46,88–94], intrinsic point defects can also modify electronic structure, carrier concentration, and hence transport properties of half-Heusler alloys [95–102]. The high-resolution angle-resolved photoemission spectroscopy (ARPES) measurements can be used to gain insights into the defect-induced changes in the electronic structure [99,103]. Controlling the precise amount of interstitial defects in the experimental samples is however a challenging task, which makes it tricky to correlate the interstitial defect concentration with the corresponding ARPES measurement. Here, we discuss the effect of the energetically favorable Ni and Co interstitials on the electronic band structure and DOS. For a systematic understanding, it is essential to study electronic structure without and with interstitial defects. Figure 3 shows *ab initio* computed electronic band structure for the four defect-free half-Heusler alloys. Our calculations predict p-type behavior for all the alloys. While these findings are in good agreement with existing theoretical results [48,85,86], experimental measurements exhibit n-type conductivity in these alloys. It is worthwhile to mention here that previous computational studies have also examined the effect of advanced approaches beyond the semilocal GGA functional such as the hybrid functional and the GW method for most of these alloys [31,52,104–106]. The GW approximation based on the many-body perturbation theory provides qualitatively similar results as that of the GGA functional with the former being more reliable, elaborate but computationally very expensive. The HSE06 hybrid functional predicted 20% to 50% larger band gap than the GGA functional for Ni-based alloys. The effect is more severe for some of the Co-based alloys where band dispersions computed with the HSE06 functional differ from the corresponding results obtained with both the GGA functional and the GW method [31]. The effect of electronic correlation on the thermoelectric properties has also been reported in several materials. This includes RuSe₂, FeSb₂, transition metal monosilicides, Co-based quaternary Heusler alloys, oxide materials, and a few half-Heusler alloys [107–115]. Nevertheless, the Ni- and Co-based half-Heusler alloys chosen in the present study are not strongly correlated electron systems and hence electronic correlation is expected to have negligible effect on our obtained results.

Next, we investigate the effect of interstitial defects on the electronic structure. Recent *ab initio* calculations focusing on the impact of interstitial Ni defects in TiNiSn revealed

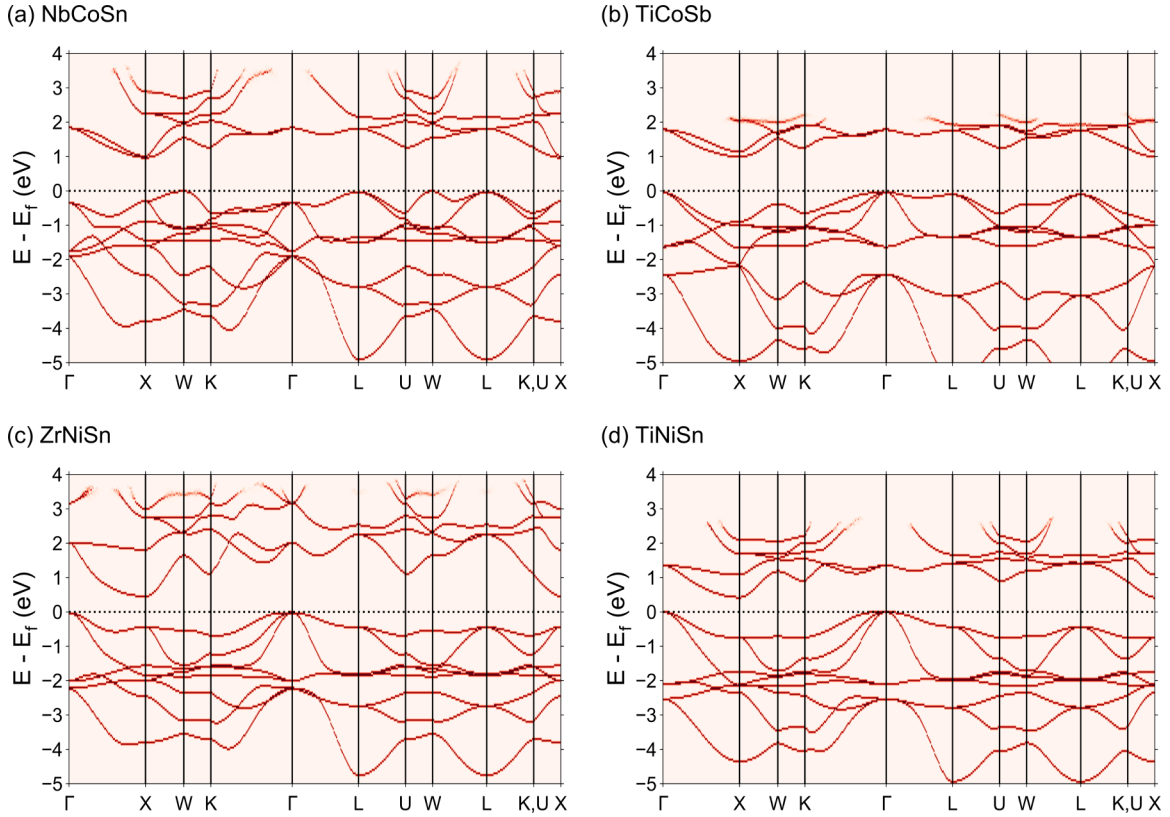


FIG. 3. Electronic band structure of ideal, defect-free (a) NbCoSn, (b) TiCoSb, (c) ZrNiSn, and (d) TiNiSn calculated using DFT. The Fermi energy (E_f) is set to 0 eV and is marked by the dotted horizontal line.

several noteworthy features in the electronic band structure and DOS [57,64,65]. The interstitial Ni leads to localized defect states close to the Fermi level within the band gap. These mid-gap defect states reduce the band gap and increase the carrier concentration of the alloy, which is likely the reason behind its attractive thermoelectric properties. Additionally, interstitial Ni defect tends to shift the Fermi level of TiNiSn in such a way that the alloy exhibits n-type nature as opposed to the p-type nature for the defect-free alloy. While these few previous investigations pointed towards the impact of interstitial defects on the electronic structure, a comprehensive understanding of the above-mentioned discrepancy between theoretical and experimental findings for several Co- and Ni-based alloys still remains elusive. Our theoretical calculations predict mid-gap states arising due to interstitial Ni defect in both the Ni-based alloys. The Fermi level also shifts closer to the conduction band indicating n-type conductivity in ZrNiSn [Fig. 4(c)] and TiNiSn [Fig. 4(d)]. Similar to Ni-containing alloys, occupation of the vacant $4d$ sites in the $C1_b$ structure by Co yields mid-gap electronic states in NbCoSn [Fig. 4(a)] and TiCoSb [Fig. 4(b)]. These mid-gap defect states in the up-spin channel of the DOS lower the band gap of Co-based alloys. An additional peak close to the Fermi level also appears in the down-spin channel. More remarkably, interstitial Co defect has similar qualitative effect on the Fermi level of NbCoSn and TiCoSb as that of interstitial Ni in the two Ni-containing alloys. In contrast to the p-type behavior of the defect-free alloys, both Co-containing alloys with interstitial Co defect exhibit n-type behavior. Our calculations thus reveal

that interstitial Ni and Co defects are pivotal in explaining the experimentally observed n-type conductivity of Ni- and Co-based half-Heusler alloys respectively.

Table I shows a comparison of our calculated band gaps, both in absence and presence of interstitial defect, with existing theoretically calculated and experimentally measured values. A key observation here is that our predicted band gap values without interstitial defect are in good agreement with previous theoretical findings for defect-free alloys. The calculated values thus obtained are significantly overestimated

TABLE I. *Ab initio* calculated band-gap values (in eV) of NbCoSn, TiCoSb, ZrNiSn, and TiNiSn without (w/o) and with interstitial defect. Previous experimentally measured and theoretically computed (w/o defect) values are also presented for comparison.

Alloy	This study (w/o defect)	This study (with defect)	Previous (calculated)	Previous (experiment)
NbCoSn	0.97	0.59	0.99 ^a	
TiCoSb	0.99	0.62	1.06 ^b	0.57 ^c
ZrNiSn	0.45	0.13	0.47 ^c	0.18 ^f
TiNiSn	0.43	0.10	0.42 ^d	0.12 ^f

^afrom Ref. [116].

^bfrom Ref. [32].

^cfrom Ref. [117].

^dfrom Ref. [65].

^efrom Ref. [118].

^ffrom Ref. [119].

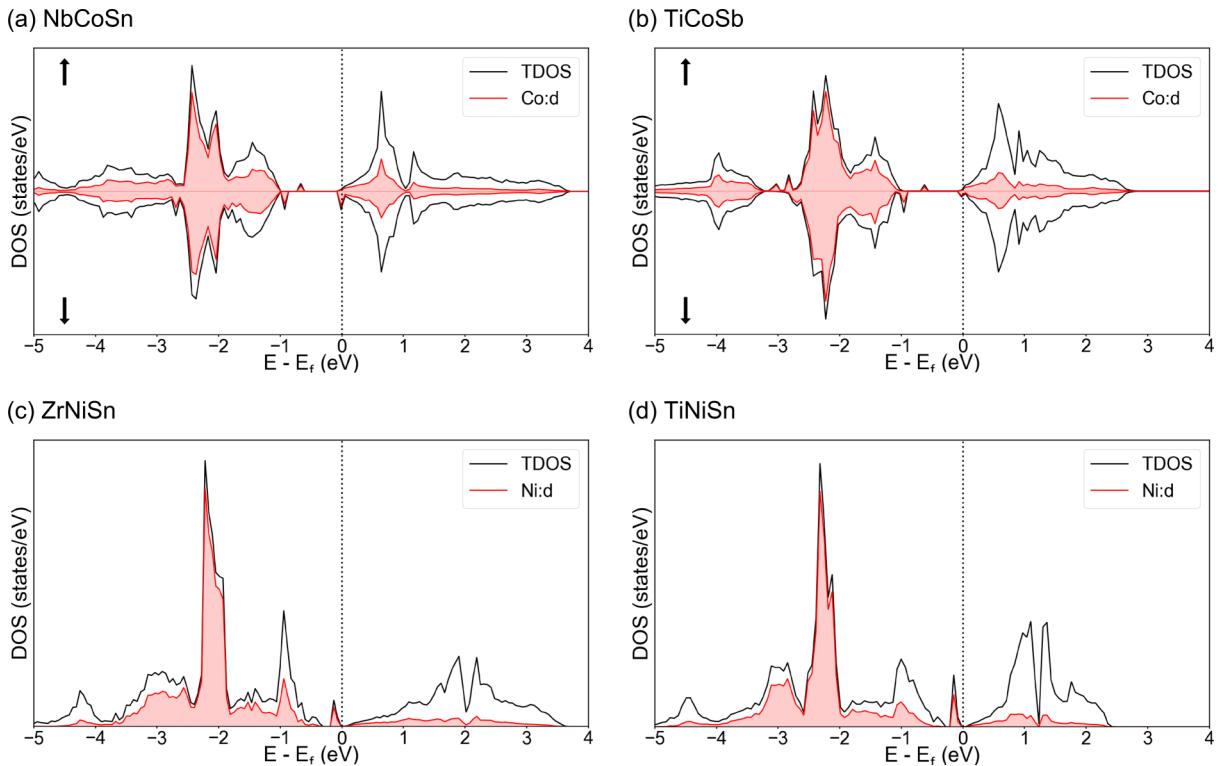


FIG. 4. Density of states (DOS) of (a) NbCoSn, (b) TiCoSb, (c) ZrNiSn, and (d) TiNiSn in presence of Co/Ni interstitial defect calculated using DFT. TDOS (black curve) corresponds to total density of states while Co:d and Ni:d (red curve) indicate d -partial density of states of Co and Ni, respectively. The \uparrow and \downarrow spins in (a) and (b) denote up-spin and down-spin channels, respectively. The Fermi energy (E_f) is set to 0 eV and is marked by the dotted vertical line.

in comparison to experimentally measured band gaps. Our calculated band gaps in the presence of interstitial defects, however, reveal significantly better agreement with the corresponding experimental values for both Co- and Ni-based alloys. Note that in the present study, we have chosen only one extra atom as defect at the interstitial site of the considered supercell. Choosing higher number of interstitial defects in theoretical simulations usually lead to the formation of cluster of defects, which may alter the predicted band-gap value and carrier concentration [64,104,120]. Hence, interstitial defects must be selected carefully in theoretical simulations in these and similar half-Heusler alloys in order to explain the experimental observation of band gap, carrier concentration, and type of electrical conductivity. We believe that the present understanding on the role of interstitial defects will help in the computational design of efficient half-Heusler alloy based thermoelectric materials with tailored properties in future.

IV. CONCLUSIONS

In conclusion, we have studied intrinsic point defects in four frequently studied n-type half-Heusler alloys, i.e., NbCoSn, TiCoSb, ZrNiSn, and TiNiSn. To this end, *ab initio* simulations have been employed to estimate defect formation energies. Our calculations reveal interstitial Ni (Co) as the

most abundant point defect in Ni-containing (Co-containing) alloys. The subsequent effect of interstitial defects on the electronic structure is found to be remarkable. In contrast to the experimental observation of n-type conductivity in these alloys, most of the previous *ab initio* studies for ideal, defect-free alloys predicted p-type behavior. Our study reveals that the presence of interstitial Ni (Co) defect brings the Fermi level closer to the conduction band in Ni-based (Co-based) alloys leading to n-type behavior and explaining the experimental observations. Furthermore, localized mid-gap states close to the Fermi level appear due to the interstitial Ni and Co defects. These defect states lower the predicted band gap and improve the agreement with the corresponding experimentally measured values. Our findings, thus, help in understanding the origin of the long-standing discrepancy between *ab initio* predicted and experimental results on the type of conductivity in these alloys. This may pave the way for using interstitial defects as a promising strategy for tailoring band gap and conductivity type, thereby helping in the design of thermoelectric materials with improved performance.

ACKNOWLEDGMENT

The authors thank Chanwon Jung and Pyuck-Pa Choi, Korea Advanced Institute of Science and Technology (KAIST), for helpful discussions.

- [1] N. L. Panwar, S. C. Kaushik, and S. Kothari, Role of renewable energy sources in environmental protection: A review, *Renew. Sustain. Energy Rev.* **15**, 1513 (2011).
- [2] T. Käberger, Progress of renewable electricity replacing fossil fuels, *Global Energy Interconn.* **1**, 48 (2018).
- [3] D. P. V. Vuuren, D. L. Bijl, P. Bogaart, E. Stehfest, H. Biemans, S. C. Dekker, J. C. Doelman, D. E. H. J. Gernaat, and M. Harmsen, Integrated scenarios to support analysis of the food–energy–water nexus, *Nat. Sustain.* **2**, 1132 (2019)
- [4] C. Forman, I. K. Muritala, R. Pardemann, and B. Meyer, Estimating the global waste heat potential, *Renew. Sustain. Energy Rev.* **57**, 1568 (2016).
- [5] L. Miró, J. Gasia, and L. F. Cabeza, Thermal energy storage (TES) for industrial waste heat (IWH) recovery: A review, *Appl. Energy* **179**, 284 (2016).
- [6] G. Schiering, Bring on the heat, *Nat. Energy* **3**, 92 (2018)
- [7] H. Jouhara, N. Khordehghah, S. Almahmoud, B. Delpech, A. Chauhan, and S. A. Tassou, Waste heat recovery technologies and applications, *Thermal Sci. Eng. Prog.* **6**, 268 (2018).
- [8] Lawrence Livermore National Laboratory, Estimated U. S. energy consumption in 2018, accessed: 4, 2020. URL <https://flowcharts.llnl.gov/commodities/energy>.
- [9] G. J. Snyder and E. S. Toberer, Complex thermoelectric materials, *Nat. Mater.* **7**, 105 (2008).
- [10] G. Chen, M. S. Dresselhaus, G. Dresselhaus, J.-P. Fleurial, and T. Caillat, Recent developments in thermoelectric materials, *Int. Mater. Rev.* **48**, 45 (2003).
- [11] A. J. Minnich, M. S. Dresselhaus, Z. F. Ren, and G. Chen, Bulk nanostructured thermoelectric materials: Current research and future prospects, *Energy Environ. Sci.* **2**, 466 (2009).
- [12] T. Varghese, C. Dun, N. Kempf, M. Saeidi-Javash, C. Karthik, J. Richardson, C. Hollar, D. Estrada, and Y. Zhang, Flexible thermoelectric devices of ultrahigh power factor by scalable printing and interface engineering, *Adv. Funct. Mater.* **30**, 1905796 (2020).
- [13] Y. Wang, L. Yang, X.-L. Shi, X. Shi, L. Chen, M. S. Dargusch, J. Zou, and Z.-G. Chen, Flexible thermoelectric materials and generators: Challenges and innovations, *Adv. Mater.* **31**, 1807916 (2019).
- [14] B. Hinterleitner, I. Knapp, M. Ponerer, Y. Shi, H. Müller, G. Eguchi, C. Eisenmenger-Sittner, M. Stöger-Pollach, Y. Kakefuda, N. Kawamoto, Q. Guo, T. Baba, T. Mori, S. Ullah, X.-Q. Chen, and E. Bauer, Thermoelectric performance of a metastable thin-film Heusler alloy, *Nature* **576**, 85 (2019).
- [15] W. Liu, J. Hu, S. Zhang, M. Deng, C.-G. Han, and Y. Liu, New trends, strategies and opportunities in thermoelectric materials: A perspective, *Mater. Today Phys.* **1**, 50 (2017).
- [16] J. Shuai, J. Mao, S. Song, Q. Zhang, G. Chen, and Z. Ren, Recent progress and future challenges on thermoelectric zintl materials, *Mater. Today Phys.* **1**, 74 (2017).
- [17] R. Gupta, N. Kumar, P. Kaur, and C. Bera, Theoretical model for predicting thermoelectric properties of tin chalcogenides, *Phys. Chem. Chem. Phys.* **22**, 18989 (2020).
- [18] W.-D. Liu, L. Yang, Z.-G. Chen, and J. Zou, Promising and eco-friendly Cu_2X -based thermoelectric materials: Progress and applications, *Adv. Mater.* **32**, 1905703 (2020).
- [19] S. Chen and Z. Ren, Recent progress of half-Heusler for moderate temperature thermoelectric applications, *Mater. Today* **16**, 387 (2013).
- [20] C. Fu, S. Bai, Y. Liu, Y. Tang, L. Chen, X. Zhao, and T. Zhu, Realizing high figure of merit in heavy-band p-type half-Heusler thermoelectric materials, *Nat. Commun.* **6**, 8144 (2015).
- [21] C. Fu, T. Zhu, Y. Liu, H. Xie, and X. Zhao, Band engineering of high performance p-type FeNbSb based half-Heusler thermoelectric materials for figure of merit $zT > 1$, *Energy Environ. Sci.* **8**, 216 (2015).
- [22] H. Zhu, R. He, J. Mao, Q. Zhu, C. Li, J. Sun, W. Ren, Y. Wang, Z. Liu, Z. Tang, A. Sotnikov, Z. Wang, D. Broido, D. J. Singh, G. Chen, K. Nielsch, and Z. Ren, Discovery of ZrCoBi based half Heuslers with high thermoelectric conversion efficiency, *Nat. Commun.* **9**, 2497 (2018).
- [23] R. A. Downie, S. A. Barczak, R. I. Smith, and J. W. G. Bos, Compositions and thermoelectric properties of XNiSn ($X = \text{Ti, Zr, Hf}$) half-Heusler alloys, *J. Mater. Chem. C* **3**, 10534 (2015).
- [24] W. G. Zeier, S. Anand, L. Huang, R. He, H. Zhang, Z. Ren, C. Wolverton, and G. J. Snyder, Using the 18-electron rule to understand the nominal 19-electron half-Heusler NbCoSb with Nb vacancies, *Chem. Mater.* **29**, 1210 (2017).
- [25] G. Joshi, X. Yan, H. Wang, W. Liu, G. Chen, and Z. Ren, Enhancement in thermoelectric figure-of-merit of an N-type half-Heusler compound by the nanocomposite approach, *Adv. Energy Mater.* **1**, 643 (2011).
- [26] W. G. Zeier, J. Schmitt, G. Hautier, U. Aydemir, Z. M. Gibbs, C. Felser, and G. J. Snyder, Engineering half-Heusler thermoelectric materials using zintl chemistry, *Nat. Rev. Mater.* **1**, 16032 (2016).
- [27] S. Bhattacharya and G. K. H. Madsen, A novel p-type half-Heusler from high-throughput transport and defect calculations, *J. Mater. Chem. C* **4**, 11261 (2016).
- [28] K. Xia, Y. Liu, S. Anand, G. J. Snyder, J. Xin, J. Yu, X. Zhao, and T. Zhu, Enhanced thermoelectric performance in 18-electron $\text{Nb}_{0.8}\text{CoSb}$ half-Heusler compound with intrinsic Nb vacancies, *Adv. Funct. Mater.* **28**, 1705845 (2018).
- [29] T. Fang, X. Zhao, and T. Zhu, Band structures and transport properties of high-performance half-Heusler thermoelectric materials by first principles, *Materials* **11**, 847 (2018).
- [30] R. A. de Groot, F. M. Mueller, P. G. van Engen, and K. H. J. Buschow, New Class of Materials: Half-Metallic Ferromagnets, *Phys. Rev. Lett.* **50**, 2024 (1983).
- [31] M. Zahedifar and P. Kratzer, Band structure and thermoelectric properties of half-Heusler semiconductors from many-body perturbation theory, *Phys. Rev. B* **97**, 035204 (2018).
- [32] S. Ouardi, G. H. Fecher, C. Felser, M. Schwall, S. S. Naghavi, A. Gloskovskii, B. Balke, J. Hamrle, K. Postava, J. Pištora, S. Ueda, and K. Kobayashi, Electronic structure and optical, mechanical, and transport properties of the pure, electron-doped, and hole-doped Heusler compound CoTiSb , *Phys. Rev. B* **86**, 045116 (2012).
- [33] H. Xie, H. Wang, C. Fu, Y. Liu, G. J. Snyder, X. Zhao, and T. Zhu, The intrinsic disorder related alloy scattering in Zr-NiSn half-Heusler thermoelectric materials, *Sci. Rep.* **4**, 6888 (2014).
- [34] S. R. Culp, J. W. Simonson, S. J. Poon, V. Ponnambalam, J. Edwards, and T. M. Tritt, (Zr, Hf)Co(Sb, Sn) half-Heusler phases as high-temperature ($> 700^\circ\text{C}$) p-type thermoelectric materials, *Appl. Phys. Lett.* **93**, 022105 (2008).

- [35] S. Bhattacharya, A. L. Pope, R. T. Littleton, T. M. Tritt, V. Ponnambalam, Y. Xia, and S. J. Poon, Effect of Sb doping on the thermoelectric properties of Ti-based half-Heusler compounds, *TiNiSn_{1-x}Sb_x*, *Appl. Phys. Lett.* **77**, 2476 (2000).
- [36] M. Zhou, C. Feng, L. Chen, and X. Huang, Effects of partial substitution of Co by Ni on the high-temperature thermoelectric properties of TiCoSb-based half-Heusler compounds, *J. Alloys Compd.* **391**, 194 (2005).
- [37] M. Zhou, L. Chen, C. Feng, D. Wang, and J.-F. Li, Moderate-temperature thermoelectric properties of TiCoSb-based half-Heusler compounds *Ti_{1-x}Ta_xCoSb*, *J. Appl. Phys.* **101**, 113714 (2007).
- [38] Y. Kimura, Y. Tamura, and T. Kita, Thermoelectric properties of directionally solidified half-Heusler compound NbCoSn alloys, *Appl. Phys. Lett.* **92**, 012105 (2008).
- [39] M. L. C. Buffon, G. Laurita, N. Verma, L. Lamontagne, L. Ghadbeigi, D. L. Lloyd, T. D. Sparks, T. M. Pollock, and R. Seshadri, Enhancement of thermoelectric properties in the Nb-Co-Sn half-Heusler/Heusler system through spontaneous inclusion of a coherent second phase, *J. Appl. Phys.* **120**, 075104 (2016).
- [40] R. He, L. Huang, Y. Wang, G. Samsonidze, B. Kozinsky, Q. Zhang, and Z. Ren, Enhanced thermoelectric properties of n-type NbCoSn half-Heusler by improving phase purity, *APL Mater.* **4**, 104804 (2016).
- [41] F. Serrano-Sánchez, T. Luo, J. Yu, W. Xie, C. Le, G. Auffermann, A. Weidenkaff, T. Zhu, X. Zhao, J. A. Alonso, B. Gault, C. Felser, and C. Fu, Thermoelectric properties of n-type half-Heusler NbCoSn with heavy-element Pt substitution, *J. Mater. Chem. A* **8**, 14822 (2020).
- [42] Y. Ono, S. Inayama, H. Adachi, and T. Kajitani, Thermoelectric properties of NbCoSn-based half-Heusler alloys, *2006 25th International Conference on Thermoelectrics, Vienna, Austria* (IEEE, Piscataway, NJ, 2006), pp. 124–127.
- [43] Q. Shen, L. Chen, T. Goto, T. Hirai, J. Yang, G. P. Meisner, and C. Uher, Effects of partial substitution of Ni by Pd on the thermoelectric properties of ZrNiSn-based half-Heusler compounds, *Appl. Phys. Lett.* **79**, 4165 (2001).
- [44] S. Sakurada and N. Shutoh, Effect of Ti substitution on the thermoelectric properties of (Zr, Hf)NiSn half-Heusler compounds, *Appl. Phys. Lett.* **86**, 082105 (2005).
- [45] C. Yu, T.-J. Zhu, R.-Z. Shi, Y. Zhang, X.-B. Zhao, and J. He, High-performance half-Heusler thermoelectric materials *Hf_{1-x}Zr_xNiSn_{1-y}Sb_y* prepared by levitation melting and spark plasma sintering, *Acta Mater.* **57**, 2757 (2009).
- [46] D. F. Zou, S. H. Xie, Y. Y. Liu, J. G. Lin, and J. Y. Li, Electronic structure and thermoelectric properties of half-Heusler *Zr_{0.5}Hf_{0.5}NiSn* by first-principles calculations, *J. Appl. Phys.* **113**, 193705 (2013).
- [47] M. K. Choudhary and P. Ravindran, Thermal, electronic and thermoelectric properties of TiNiSn and TiCoSb based quaternary half Heusler alloys obtained from *ab initio* calculations, *Sustain. Energy Fuels* **4**, 895 (2020).
- [48] L. L. Wang, L. Miao, Z. Y. Wang, W. Wei, R. Xiong, H. J. Liu, J. Shi, and X. F. Tang, Thermoelectric performance of half-Heusler compounds TiNiSn and TiCoSb, *J. Appl. Phys.* **105**, 013709 (2009).
- [49] C. S. Birkel, W. G. Zeier, J. E. Douglas, B. R. Lettiere, C. E. Mills, G. Seward, A. Birkel, M. L. Snedaker, Y. Zhang, G. J. Snyder, T. M. Pollock, R. Seshadri, and G. D. Stucky, Rapid microwave preparation of thermoelectric TiNiSn and TiCoSb half-Heusler compounds, *Chem. Mater.* **24**, 2558 (2012).
- [50] C. S. Birkel, J. E. Douglas, B. R. Lettiere, G. Seward, N. Verma, Y. Zhang, T. M. Pollock, R. Seshadri, and G. D. Stucky, Improving the thermoelectric properties of half-Heusler TiNiSn through inclusion of a second full-Heusler phase: Microwave preparation and spark plasma sintering of *TiNi_{1+x}Sn*, *Phys. Chem. Chem. Phys.* **15**, 6990 (2013).
- [51] M. Gürth, G. Rogl, V. V. Romaka, A. Grytsiv, E. Bauer, and P. Rogl, Thermoelectric high ZT half-Heusler alloys *Ti_{1-x-y}Zr_xHf_yNiSn* ($0 \leq x \leq 1$; $0 \leq y \leq 1$), *Acta Mater.* **104**, 210 (2016).
- [52] Y. G. Yu, X. Zhang, and A. Zunger, Natural off-stoichiometry causes carrier doping in half-Heusler filled tetrahedral structures, *Phys. Rev. B* **95**, 085201 (2017).
- [53] A. Tavassoli, A. Grytsiv, G. Rogl, V. V. Romaka, H. Michor, M. Reissner, E. Bauer, M. Zehetbauer, and P. Rogl, The half Heusler system *Ti_{1+x}Fe_{1.33-x}Sb-TiCoSb* with Sb/Sn substitution: Phase relations, crystal structures and thermoelectric properties, *Dalton Trans.* **47**, 879 (2018).
- [54] K. Kirievsky, Y. Gelbstein, and D. Fuks, Phase separation and antisite defects in the thermoelectric tinisn half-Heusler alloys, *J. Solid State Chem.* **203**, 247 (2013).
- [55] M. Wambach, R. Stern, S. Bhattacharya, P. Ziolkowski, E. Müller, G. K. H. Madsen, and A. Ludwig, Unraveling self-doping effects in thermoelectric TiNiSn half-Heusler compounds by combined theory and high-throughput experiments, *Adv. Electron. Mater.* **2**, 1500208 (2016).
- [56] Y. Tang, X. Li, L. H. J. Martin, E. C. Reyes, T. Ivas, C. Leinenbach, S. Anand, M. Peters, G. J. Snyder, and C. Battaglia, Impact of Ni content on the thermoelectric properties of half-Heusler tinisn, *Energy Environ. Sci.* **11**, 311 (2018).
- [57] M. Rittiruum, A. Yangthaisong, and T. Seetawan, Enhancing the thermoelectric performance of self-defect TiNiSn: A first-principles calculation, *J. Electron. Mater.* **47**, 7456 (2018).
- [58] V. V. Romaka, P. Rogl, L. Romaka, Yu. Stadnyk, A. Grytsiv, O. Lakh, and V. Krayovskii, Peculiarities of structural disorder in Zr- and Hf-containing Heusler and half-Heusler stannides, *Intermetallics* **35**, 45 (2013).
- [59] M. N. Guzik, C. Echevarria-Bonet, M. D. Riktor, P. A. Carvalho, A. E. Gunnæs, M. H. Sørby, and B. C. Hauback, Half-Heusler phase formation and Ni atom distribution in M-Ni-Sn (M = Hf, Ti, Zr) systems, *Acta Mater.* **148**, 216 (2018).
- [60] H.-H. Xie, J.-L. Mi, L.-P. Hu, N. Lock, M. Chirstensen, C.-G. Fu, B. B. Iversen, X.-B. Zhao, and T.-J. Zhu, Interrelation between atomic switching disorder and thermoelectric properties of ZrNiSn half-Heusler compounds, *CrystEngCommun* **14**, 4467 (2012).
- [61] M. Schrade, K. Berland, A. Kosinskiy, J. P. Heremans, and T. G. Finstad, Shallow impurity band in ZrNiSn, *J. Appl. Phys.* **127**, 045103 (2020).
- [62] H. J. Goldsmid and J. W. Sharp, Estimation of the thermal band gap of a semiconductor from seebeck measurements, *J. Electron. Mater.* **28**, 869 (1999).
- [63] S. Barczak, J. Buckman, R. Smith, A. Baker, E. Don, I. Forbes, and J.-W. Bos, Impact of interstitial Ni on the thermoelectric properties of the half-Heusler TiNiSn, *Materials* **11**, 536 (2018).

- [64] J. E. Douglas, P. A. Chater, C. M. Brown, T. M. Pollock, and R. Seshadri, Nanoscale structural heterogeneity in Ni-rich half-Heusler TiNiSn, *J. Appl. Phys.* **116**, 163514 (2014).
- [65] C. Colinet, P. Jund, and J.-C. Tédénac, NiTiSn a material of technological interest: Ab initio calculations of phase stability and defects, *Intermetallics* **46**, 103 (2014).
- [66] P. Hohenberg and W. Kohn, Inhomogeneous electron gas, *Phys. Rev.* **136**, B864 (1964).
- [67] W. Kohn and L. J. Sham, Self-consistent equations including exchange and correlation effects, *Phys. Rev.* **140**, A1133 (1965).
- [68] G. Kresse and J. Hafner, Ab initio molecular dynamics for open-shell transition metals, *Phys. Rev. B* **48**, 13115 (1993).
- [69] G. Kresse and J. Furthmüller, Efficient iterative schemes for *ab initio* total-energy calculations using a plane-wave basis set, *Phys. Rev. B* **54**, 11169 (1996).
- [70] G. Kresse and J. Furthmüller, Efficiency of ab-initio total energy calculations for metals and semiconductors using a plane-wave basis set, *Comput. Mater. Sci.* **6**, 15 (1996).
- [71] P. E. Blöchl, Projector augmented-wave method, *Phys. Rev. B* **50**, 17953 (1994).
- [72] J. P. Perdew, K. Burke, and M. Ernzerhof, Generalized Gradient Approximation Made Simple, *Phys. Rev. Lett.* **77**, 3865 (1996).
- [73] P. E. Blöchl, O. Jepsen, and O. K. Andersen, Improved tetrahedron method for brillouin-zone integrations, *Phys. Rev. B* **49**, 16223 (1994).
- [74] C. Freysoldt, B. Grabowski, T. Hickel, J. Neugebauer, G. Kresse, A. Janotti, and C. G. Van de Walle, First-principles calculations for point defects in solids, *Rev. Mod. Phys.* **86**, 253 (2014).
- [75] H. Hazama, M. Matsubara, R. Asahi, and T. Takeuchi, Improvement of thermoelectric properties for half-Heusler tinin by interstitial Ni defects, *J. Appl. Phys.* **110**, 063710 (2011).
- [76] M. L. C. Buffon, G. Laurita, L. Lamontagne, E. E. Levin, S. Mooraj, D. L. Lloyd, N. White, T. M. Pollock, and R. Seshadri, Thermoelectric performance and the role of anti-site disorder in the 24-electron Heusler TiFe₂Sn, *J. Phys.: Condens. Matter* **29**, 405702 (2017).
- [77] V. Popescu, P. Kratzer, S. Wimmer, and H. Ebert, Native defects in the Co₂TiZ (Z = Si, Ge, Sn) full Heusler alloys: Formation and influence on the thermoelectric properties, *Phys. Rev. B* **96**, 054443 (2017).
- [78] S. Anand, R. Gurunathan, T. Soldi, L. Borgsmiller, R. Orenstein, and G. J. Snyder, Thermoelectric transport of semiconductor full-Heusler VFe₂Al, *J. Mater. Chem. C* **8**, 10174 (2020).
- [79] J. Park, Y. Xia, A. M. Ganose, A. Jain, and V. Ozoliņš, High Thermoelectric Performance and Defect Energetics of Multipocketed Full Heusler Compounds, *Phys. Rev. Applied* **14**, 024064 (2020).
- [80] J. P. Perdew, Density functional theory and the band gap problem, *Int. J. Quantum Chem.* **28**, 497 (1985).
- [81] A. Seidl, A. Görling, P. Vogl, J. A. Majewski, and M. Levy, Generalized Kohn-Sham schemes and the band-gap problem, *Phys. Rev. B* **53**, 3764 (1996).
- [82] P. A. Schultz, Theory of Defect Levels and the “Band Gap Problem” in Silicon, *Phys. Rev. Lett.* **96**, 246401 (2006).
- [83] M. K. Y. Chan and G. Ceder, Efficient Band Gap Prediction for Solids, *Phys. Rev. Lett.* **105**, 196403 (2010).
- [84] J. P. Perdew, W. Yang, K. Burke, Z. Yang, E. K. U. Gross, M. Scheffler, G. E. Scuseria, T. M. Henderson, I. Y. Zhang, A. Ruzsinszky, H. Peng, J. Sun, E. Trushin, and A. Görling, Understanding band gaps of solids in generalized Kohn–Sham theory, *Proc. Natl. Acad. Sci. USA* **114**, 2801 (2017).
- [85] S. Ögüt and K. M. Rabe, Band gap and stability in the ternary intermetallic compounds NiSnM (M=Ti, Zr, Hf): A first-principles study, *Phys. Rev. B* **51**, 10443 (1995).
- [86] S. Ouardi, G. H. Fecher, B. Balke, X. Kozina, G. Stryganyuk, C. Felser, S. Lowitzer, D. Ködderitzsch, H. Ebert, and E. Ikenaga, Electronic transport properties of electron- and hole-doped semiconducting C1_b Heusler compounds: NiTi_{1-x}M_xSn (M = Sc, V), *Phys. Rev. B* **82**, 085108 (2010).
- [87] M. Hichour, D. Rached, R. Khenata, M. Rabah, M. Merabet, A. H. Reshak, S. B. Omran, and R. Ahmed, Theoretical investigations of NiTiSn and CoVSn compounds, *J. Phys. Chem. Solids* **73**, 975 (2012).
- [88] K. Kawano, K. Kurosaki, T. Sekimoto, H. Muta, and S. Yamanaka, Effect of Sn doping on the thermoelectric properties of ernisb-based p-type half-Heusler compound, *Appl. Phys. Lett.* **91**, 062115 (2007).
- [89] H. Muta, T. Kanemitsu, K. Kurosaki, and S. Yamanaka, High-temperature thermoelectric properties of Nb-doped MNiSn (M=Ti, Zr) half-Heusler compound, *J. Alloys Compd.* **469**, 50 (2009).
- [90] C. Fu, Y. Liu, H. Xie, X. Liu, X. Zhao, G. Jeffrey Snyder, J. Xie, and T. Zhu, Electron and phonon transport in codoped FeV_{0.6}Nb_{0.4}Sb half-Heusler thermoelectric materials, *J. Appl. Phys.* **114**, 134905 (2013).
- [91] O. Appel and Y. Gelbstein, A comparison between the effects of Sb and Bi doping on the thermoelectric properties of the Ti_{0.3}Zr_{0.35}Hf_{0.35}NiSn half-Heusler alloy, *J. Electron. Mater.* **43**, 1976 (2014).
- [92] L. Huang, Q. Zhang, Y. Wang, R. He, J. Shuai, J. Zhang, C. Wang, and Z. Ren, The effect of Sn doping on thermoelectric performance of n-type half-Heusler NbCoSb, *Phys. Chem. Chem. Phys.* **19**, 25683 (2017).
- [93] N. Farahi, C. Stiewe, D. Y. N. Truong, Y. Shi, S. Salamon, J. Landers, B. Eggert, H. Wende, J. de Boor, H. Kleinke, and E. Müller, Effects of Ta substitution on the microstructure and transport properties of Hf-doped NbFeSb half-Heusler thermoelectric materials, *ACS Appl. Energy Mater.* **2**, 8244 (2019).
- [94] B. Gong, F. Liu, J. Zhu, X. Wang, W. Ao, C. Zhang, Y. Li, J. Li, and H. Xie, Effects of Sc, Ti, Hf, V, Nb and Ta doping on the properties of ZrNiSn alloys, *J. Mater. Sci.* **54**, 10325 (2019).
- [95] K. Miyamoto, A. Kimura, K. Sakamoto, M. Ye, Y. Cui, K. Shimada, H. Namatame, M. Taniguchi, S. ichi Fujimori, Y. Saitoh, E. Ikenaga, K. Kobayashi, J. Tadano, and T. Kanomata, In-gap electronic states responsible for the excellent thermoelectric properties of Ni-based half-Heusler alloys, *Appl. Phys. Express* **1**, 081901 (2008).
- [96] Y. W. Chai, K. Yoshioka, and Y. Kimura, Intrinsic point defects in thermoelectric half-Heusler alloys, *Scr. Mater.* **83**, 13 (2014).
- [97] A. Berche and P. Jund, Fully ab-initio determination of the thermoelectric properties of half-Heusler NiTiSn: Crucial role of interstitial Ni defects, *Materials* **11**, 868 (2018).

- [98] W. Ren, H. Zhu, J. Mao, L. You, S. Song, T. Tong, J. Bao, J. Luo, Z. Wang, and Z. Ren, Manipulation of Ni interstitials for realizing large power factor in TiNiSn-based materials, *Adv. Electron. Mater.* **5**, 1900166 (2019).
- [99] C. Fu, M. Yao, X. Chen, L. Z. Maulana, X. Li, J. Yang, K. Imasato, F. Zhu, G. Li, G. Auffermann, U. Burkhardt, W. Schnelle, J. Zhou, T. Zhu, X. Zhao, M. Shi, M. Dressel, A. V. Pronin, G. J. Snyder, and C. Felser, Revealing the intrinsic electronic structure of 3d half-Heusler thermoelectric materials by angle-resolved photoemission spectroscopy, *Adv. Sci.* **7**, 1902409 (2020).
- [100] Y. Sun, W. Qiu, L. Zhao, H. He, L. Yang, L. Chen, H. Deng, X. Shi, and J. Tang, Defects engineering driven high power factor of ZrNiSn-based half-Heusler thermoelectric materials, *Chem. Phys. Lett.* **755**, 137770 (2020).
- [101] T. C. Chibueze, A. T. Raji, and C. M. I. Okoye, Intrinsic point defects in half-Heusler AuMnSn, *J. Phys. Chem. Solids* **139**, 109328 (2020).
- [102] H. Miyazaki, O. M. Ozkendir, S. Gunaydin, K. Watanabe, K. Soda, and Y. Nishino, Probing local distortion around structural defects in half-Heusler thermoelectric NiZrSn alloy, *Sci. Rep.* **10**, 19820 (2020).
- [103] Z. K. Liu, L. X. Yang, S.-C. Wu, C. Shekhar, J. Jiang, H. F. Yang, Y. Zhang, S.-K. Mo, Z. Hussain, B. Yan, C. Felser, and Y. L. Chen, Observation of unusual topological surface states in half-Heusler compounds LnPtBi (Ln=Lu, Y), *Nat. Commun.* **7**, 12924 (2016).
- [104] D. T. Do, S. D. Mahanti, and J. J. Pulikkoti, Electronic structure of Zr-Ni-Sn systems: Role of clustering and nanostructures in half-Heusler and Heusler limits, *J. Phys.: Condens. Matter* **26**, 275501 (2014).
- [105] G. Fiedler and P. Kratzer, Ternary semiconductors nizrsn and cozrbi with half-Heusler structure: A first-principles study, *Phys. Rev. B* **94**, 075203 (2016).
- [106] K. Berland, N. Shulumba, O. Hellman, C. Persson, and O. M. Løvvik, Thermoelectric transport trends in group 4 half-Heusler alloys, *J. Appl. Phys.* **126**, 145102 (2019).
- [107] K. Wang, A. Wang, A. Tomic, L. Wang, A. M. M. Abeykoon, E. Dooryhee, S. J. L. Billinge, and C. Petrovic, Enhanced thermoelectric power and electronic correlations in RuSe₂, *APL Mater.* **3**, 041513 (2015).
- [108] K. Wang, R. Hu, J. Warren, and C. Petrovic, Enhancement of the thermoelectric properties in doped FeSb₂ bulk crystals, *J. Appl. Phys.* **112**, 013703 (2012).
- [109] P. Sun, N. Oeschler, S. Johnsen, B. B. Iversen, and F. Steglich, Huge thermoelectric power factor: FeSb₂ versus FeAs₂ and RuSb₂, *Appl. Phys. Express* **2**, 091102 (2009).
- [110] A. Sakai, F. Ishii, Y. Onose, Y. Tomioka, S. Yotsuhashi, H. Adachi, N. Nagaosa, and Y. Tokura, Thermoelectric power in transition-metal monosilicides, *J. Phys. Soc. Jpn.* **76**, 093601 (2007).
- [111] J. M. Tomczak, K. Haule, and G. Kotliar, Signatures of electronic correlations in iron silicide, *Proc. Natl. Acad. Sci. USA* **109**, 3243 (2012).
- [112] A. Q. Seh and D. C. Gupta, Exploration of highly correlated co-based quaternary Heusler alloys for spintronics and thermoelectric applications, *Int. J. Energy Res.* **43**, 8864 (2019).
- [113] Y. Ando, N. Miyamoto, K. Segawa, T. Kawata, and I. Terasaki, Specific-heat evidence for strong electron correlations in the thermoelectric material (Na, Ca)Co₂O₄, *Phys. Rev. B* **60**, 10580 (1999).
- [114] S. Balamurugan, K. Yamaura, A. B. Karki, D. P. Young, M. Arai, and E. Takayama-Muromachi, Specific-heat evidence of strong electron correlations and thermoelectric properties of the ferromagnetic perovskite SrCoO_{3-δ}, *Phys. Rev. B* **74**, 172406 (2006).
- [115] E. H. Shourov, P. J. Strohbeen, D. Du, A. Sharan, F. C. de Lima, F. Rodolakis, J. L. McChesney, V. Yannello, A. Janotti, T. Birol, and J. K. Kawasaki, Electronic correlations in the semiconducting half-Heusler compound FeVSb, *Phys. Rev. B* **103**, 045134 (2021).
- [116] L. Xi, J. Yang, L. Wu, J. Yang, and W. Zhang, Band engineering and rational design of high-performance thermoelectric materials by first-principles, *J. Materiomics* **2**, 114 (2016).
- [117] K. K. Johari, R. Bhardwaj, N. S. Chauhan, B. Gahtori, S. Bathula, S. Auluck, and S. R. Dhakate, Band structure modification and mass fluctuation effects of isoelectronic germanium-doping on thermoelectric properties of ZrNiSn, *ACS Appl. Energy Mater.* **3**, 1349 (2020).
- [118] P. Qiu, X. Huang, X. Chen, and L. Chen, Enhanced thermoelectric performance by the combination of alloying and doping in TiCoSb-based half-Heusler compounds, *J. Appl. Phys.* **106**, 103703 (2009).
- [119] F. G. Aliev, V. V. Kozyrkov, V. V. Moshchalkov, R. V. Scolozdra, and K. Durczewski, Narrow band in the intermetallic compounds MNiSn (M=Ti, Zr, Hf), *Z. Phys. B: Condens. Matter* **80**, 353 (1990).
- [120] C. Jung, B. Dutta, P. Dey, S. J. Jeon, S. Han, H.-M. Lee, J.-S. Park, S.-H. Yi, and P.-P. Choi, Tailoring nanostructured NbCoSn-based thermoelectric materials via crystallization of an amorphous precursor, *Nano Energy* **80**, 105518 (2021).